

Analysis of Ti-6Al-4V Implants Placed with Fibroblast Growth Factor 1 in Rat Tibiae

Michael McCracken, DDS, PhD¹/Jack E. Lemons, PhD²/Kurt Zinn, DVM, PhD³

Titanium-aluminum-vanadium (Ti-6Al-4V) implants were placed in the tibiae of 32 rats (male Sprague-Dawley, 350 g) to examine healing and bone response. Half of the implants were treated with fibroblast growth factor 1 (FGF-1) delivered in an activated fibrinogen matrix. Animals were injected with a radiopharmaceutical imaging agent, technetium-99m-methylene diphosphonate (Tc-99m-MDP), which concentrates in bone, especially in areas of higher osteoblastic activity. Binding of Tc-99m-MDP to the implant was detected in vivo by Anger gamma camera imaging. Fourteen days after implant surgery, specimens were recovered and prepared for histomorphometric analysis. Histologic examination revealed that samples treated with FGF-1 demonstrated significantly greater amounts of bone-to-implant contact ($P < .05$) compared to controls. Also, FGF-1-treated samples showed significantly greater amounts of bone (percent volume) adjacent to implants ($P < .005$). These findings were supported by analyses of the non-invasive Tc-99m-MDP images, which demonstrated significantly greater uptake of Tc-99m-MDP adjacent to FGF-1-treated implants ($P < .05$). Results of the experiments supported the hypothesis that FGF-1 could increase bone production around implants in a rat model. (INT J ORAL MAXILLOFAC IMPLANTS 2001;16:495-502)

Key words: dental implants, fibroblast growth factor, osseointegration, radioimmunodetection

Dental implants continue to provide a predictable and viable treatment option for patients missing teeth.¹⁻⁵ Many patients turn to dental implants for oral rehabilitation, often because they have unsuccessfully worn a conventional removable denture or they desire a more stable or fixed prosthesis. After a healing period, the implants may be restored with a fixed or removable prosthesis, with an associated increase in chewing ability, function, esthetics, and phonetics. Unfortunately, the total treatment time for some patients may exceed 12 months.⁶

In an attempt to improve this current condition, researchers have worked to enhance the healing rate and bone density around endosseous implants. One

possible method to enhance tissue response is to manipulate the host site with growth factors or other cytokines. A variety of substances, including platelet-derived growth factor (PDGF), insulin-like growth factor (IGF), and bone morphogenetic proteins (BMPs), have been studied.⁷⁻¹⁷

Fibroblast growth factors (FGF) have also been shown to increase bone activity and bone healing. The subgroups FGF-1 and FGF-2 have received the most study in this area. These studies are summarized in Table 1. However, there is little research that examines the effects of FGF on healing adjacent to dental implant materials, such as titanium or titanium alloy. Much more has been written, for example, about the interactions of BMP with these materials. Even less appears in the literature regarding a specific subgroup of the FGF family, FGF-1.

It is reasonable to believe that the addition of FGF-1 could enhance healing around titanium implants, in that FGF-1 and FGF-2 are potent cell mediators. Originally, this cytokine was labeled "fibroblast" growth factor because its effects were first noted on fibroblast cells. It is now known that the effects of FGF are not limited to fibroblasts. Fibroblast growth factors are mitogenic for mesodermal, neuroectodermal, and endodermal cell types, and in vitro actions include modulation of

¹Assistant Professor, Department of Prosthodontics and Biomaterials, University of Alabama School of Dentistry, Birmingham, Alabama.

²Professor, Department of Prosthodontics and Biomaterials, University of Alabama School of Dentistry, Birmingham, Alabama.

³Associate Professor, Department of Radiology, University of Alabama, Birmingham, Alabama.

Reprint requests: Dr Michael McCracken, Department of Prosthodontics and Biomaterials, SDB 49, University of Alabama School of Dentistry, 1530 3rd Avenue South, Birmingham, AL 35294-0007. Fax: (205) 975-6108. E-mail: mikemc@uab.edu

Table 1 Summary of Literature Reporting Effects of FGF on Bone Growth or Osteogenic-type Cells

Study	FGF	Model	Results
Wang and Aspenberg 1996 ³⁰	FGF-2	Rat	Biphasic response; at optimal dose, bone associated with titanium chambers increases
Aspenberg et al 1989 ³¹	FGF-2	Rat	FGF in gel carrier increases bone formation in demineralized bone implants; FGF alone had no result
Schliephake et al 1998 ³²	FGF-2	Miniature pig	Single dose of FGF (no carrier) produces no increase in bone
Wiltfang and Merten 1996 ³³	FGF-2	Miniature pig	FGF increases bone production by angiogenesis and cell recruitment
Rodan et al 1987 ³⁴	FGF-1	Culture	FGF stimulates rat osteoblastic cells
Bland et al 1995 ³⁵	FGF-1, FGF-2	Rabbit	FGF administered in single dose (no releasing agent) has no effect on bone
Nakamura et al 1995 ³⁶	FGF-2	Rat	Systemic injections of FGF stimulate generalized bone growth
Mayahara et al 1993 ³⁷	FGF-1, FGF-2	Rat	Systemic injections of FGF show increase in bone production and calcium content of long bones

cell motility and differentiation.¹⁸ They also stabilize phenotypic expression of cultured cells and delay cell senescence.¹⁹ Importantly, FGFs increase angiogenesis *in vivo* and may play a crucial role in wound healing.¹⁹⁻²¹

Implant Imaging

As the need for biomimetic and bioengineering materials increases, so does the need for research tools to evaluate host response. Gamma camera imaging with biologically active radiotracers offers many possibilities in this area. A specific example of this technology is *in vivo* imaging with technetium-99m-methylene diphosphonate (Tc-99m-MDP). This substance has been used in a variety of situations to examine bone and bone growth, and it is approved for human use as a diagnostic tool for metastasis of cancer to bone. Its potential as a research tool, however, especially for small animal models, has not been fully developed.

Technetium-99m is a radioactive isotope with a half-life of 6 hours, and in various chemical forms it accounts for approximately 90% of all nuclear medicine scans. Advantages include its relatively short half-life, high abundance of 140 keV gamma ray emission (89%), and lack of β emission. Many consider Tc-99m to be less dangerous than other radioisotopes commonly used in medical research and ideal for noninvasive imaging. It can be used in any laboratory that utilizes standard radiation hygiene protocols.

Few published articles apply radioimaging technology to the study of implant healing with growth

factors or other bioengineering materials. Some have reported the use of scintimetric techniques, but this involved harvesting of the tissue.^{22,23} Many advantages could exist for *in vivo* imaging techniques that do not require sacrifice of the host animal. For example, studies could be done over time, including multiple within-subject comparisons. The effect of drugs or other biologically active agents could be assessed in different combinations. Gamma camera imaging with Tc-99m-MDP provides such a research tool.

In this investigation, the following hypotheses were tested: First, titanium alloy implants (Ti-6Al-4V) placed with FGF-1 would show an increased quantity of associated bone compared to implants alone; second, Ti-6Al-4V implants placed with FGF-1 would result in greater uptake of Tc-99m-MDP radioactivity than implants placed alone, and the difference could be measured by noninvasive imaging.

MATERIALS AND METHODS

Animals were maintained in an AAALAC-accredited (American Association for Accreditation of Laboratory Animal Care) animal care and use program in accordance with the standards of the Guide for the Care and Use of Laboratory Animals (NRC 1996). Thirty-two male Sprague-Dawley rats weighing 350 to 375 g (4 months old) were divided into test and control groups of 16 each. The test group received implants treated with FGF-1 in an

activated fibrinogen matrix. The control group received implants only.

Rats were anesthetized with volatile gas (enflurane), shaved, scrubbed, and draped to present a surgical field. A 1.5-cm incision was made on the medial-proximal surface of the tibia above the tibial protuberance. Tissue was reflected to expose the flat portion of the tibia below the knee. Using a slow-speed surgical handpiece (Nobel Biocare, Yorba Linda, CA) with a No. 4 round bur and copious warm saline irrigation, a pilot hole was drilled in the tibia 8 mm proximal to the tibial protuberance. A 1.3-mm-diameter surgical implant drill was used to create an oblique-transverse osteotomy, traveling through the medullary canal and the opposite cortical plate. Rather than drilling perpendicular to the bone, the oblique path of implant placement was used to optimize the implant surface area for each specimen (Fig 1). A No. 6 round bur was used to increase the size of the hole in the medial aspect of the tibia. The osteotomy was irrigated with 20 mL of warm saline.

Titanium alloy screws measuring 1.5×8 mm were obtained for implantation (Walter Lorenz Surgical, Jacksonville, FL). Implants were placed manually. The implant engaged the opposite cortical plate but did not engage the medial cortical plate, which had been enlarged with the No. 6 round bur. The test group was treated by injecting 65 μ g of FGF-1 (16 μ L) in an activated fibrin matrix. This matrix was formed by mixing the FGF-1 with 0.1 units of thrombin (20 μ L) (Sigma-Aldrich, St. Louis, MO) and 0.6 mg of fibrinogen (60 μ L) (Sigma-Aldrich). The thrombin and fibrinogen liquids formed a gel-like mass after 2 minutes. The FGF-1 was mixed with the thrombin and fibrinogen and injected into the osteotomy before setting occurred.

The dose, sample size, and matrix formula had been determined previously in pilot and related studies. It was determined that a 65- μ g dose of FGF-1 increased healing in a rat model with hydroxyapatite powder; so that dose was used for this study. Samples were examined at day 14, because this is the midpoint in healing for this species, which is essentially finished after 28 days²⁴; this provides an examination where bone is present but still developing. In a pilot study, implants placed with the fibrinogen matrix alone were not statistically different from controls with implants alone. Therefore, the control group received implants alone to simplify surgical procedures.

Primary closure was achieved for each animal by approximating the muscle layers with sutures and closing the skin with surgical staples. Approximately

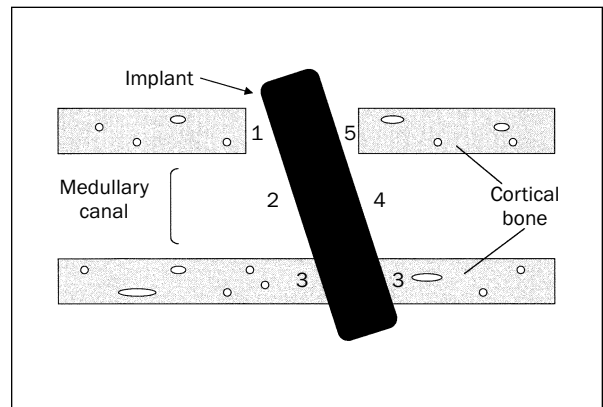


Fig 1 Schematic of implant placed in rat tibia. Zone 1 is the proximal portion of the medial cortical plate. Zone 2 is the proximal medullary canal. Zone 3 is the opposite cortical plate (proximal and distal aspects). Zone 4 is the distal medullary canal. Zone 5 is the distal portion of the cortical plate.

200 μ L of blood was obtained from each animal using a tail snip. Hemostasis was achieved with a cauterizer. Blood samples were left at room temperature for 1 hour and spun, and serum was extracted and frozen. All rats recovered from surgery and displayed normal mobility and activity after 1 or 2 hours. Rats received standard rodent chow and water ad libitum.

Analysis by Tc-99m-MDP

After 5 days, a subset of 12 rats was imaged after injection with Tc-99m-MDP. Rats were anesthetized using volatile gas. The Tc-99m-MDP was obtained from the Central Pharmacy (Birmingham, AL). Approximately 1700 μ Ci of activity was drawn into a tuberculin syringe and diluted to 200 μ L with saline. Activity was measured with a dose calibrator (Atomlab 100, Biodex Medical Systems, Shirley, NY). The Tc-99m-MDP was administered intravenously into the penile vein of the rats. This location was selected because it is readily accessible and is easily visualized to ensure intravenous injection of the radiotracer. Activity in the syringe was again measured, and the difference before and after injection was considered the actual dose. Animals received approximately 1,500 μ Ci of Tc-99m-MDP.

After waiting for 3 hours to allow the Tc-99m-MDP to clear the soft tissue and be excreted, rats were anesthetized and imaged (static, planar technique) using an Anger 420/550 mobile radioisotope gamma camera (Technicare, Sulon, OH). Two images were collected: a whole-body image and a leg image. The whole-body images were collected over 60 seconds (50,000 counts) using a high-resolution parallel-hole collimator. A close-up image of the leg joint and implant healing site was then collected

over a period of 300 seconds (50,000 counts) using a pinhole collimator. In this case, the end of the cone was about 4 cm from the joint space.

Images were analyzed using a modified version of NIH Image software (NucMed Image, Mark D. Wittry, University of Saint Louis, MO). Region-of-interest analyses were conducted on each image by drawing a circle around the area of increased bone activity around each implant and recording counts in the area, as well as the number of pixels in the area. The value is reported as Tc-99m density, or mean counts/pixel.

Two areas were measured on each animal: the proximal half of the cranium (whole-body image) and the implant area (implant image). A baseline absorption factor was determined from measuring the cranium to compensate for variables associated with the procedure, such as dose of Tc-99m-MDP, differences in clearing rates, bone density variations, animal size, and metabolism. The cranial values were averaged, and then each individual animal was normalized to the average value. Counts associated with implants were multiplied by this normalization coefficient to determine the adjusted activity for each implant area.

Histomorphometric Analysis

After 14 days, rats were euthanized with carbon dioxide inhalation. Tibiae were removed, cleaned of soft tissue, and fixed in phosphate-buffered paraformaldehyde for 12 hours. Specimens were dehydrated with progressive alcohols under vacuum over 14 days, cleared with xylene, and infiltrated and embedded with Technovit 7200 (Exakt Technologies, Oklahoma City, OK). Samples were prepared for light microscopy by cutting and grinding techniques described by Donath and Breuner²⁵ using an Exakt cutting and grinding system (Exakt Technologies). Final sample slide thickness was less than 60 μm ; slides were stained with toluidine blue, which stains new bone a darker blue than existing bone.

Samples were examined for histomorphometric analysis using an imaging system and microcomputer analysis. Briefly, a Sony 3-chip charge-coupled device videocamera (Sony Corporation of America, New York, NY) fed live images to a microcomputer, which captured the images with a video capture board (Scion Corporation, Frederick, MD). These images were analyzed using modified NIH image software (Scion Corporation).

Three different histomorphometric quantities were determined for each sample: percent bone-to-implant contact, bone volume percent around the implant, and frequency of bone contact along the implant surface. Each of these quantities is defined as follows.

- Bone-to-implant contact was measured in 5 zones around the implants. Percent contact (linear contact) was defined as the length of bone contacting the implant, divided by the length of the implant. Bone contact was defined as no visible gap at the light microscopic level; for this system, this represents any bone within 10 μm of the implant surface.
- Bone volume percent was defined as the amount of bone within 1.5 mm of the implant surface, divided by the area of that region. Bone was identified by thresholding and digitizing techniques to minimize operator error. Bone volume was measured around the proximal cortical area of the implant (zones 1 and 5) and the medullary region (zones 2 and 4) (see Fig 1).
- Total count/frequency of contact was the number of bone nodules (areas of calcification) that were touching the implant. This is an integer for each implant and measures the frequency of contact, rather than volume or length of bone.

Statistical Analysis

Statistics were performed using StatView software (SAS Institute, Cary, NC). Comparisons of different measurements between groups were analyzed using multivariate analysis of variance (MANOVA). Since this test indicated a significant difference among groups, particular areas of analysis were examined with the Fisher PLSD post hoc analysis. Results were considered significant at the $\alpha = .05$ level.

RESULTS

Specimens were examined using a light microscope at 40 \times and 100 \times magnifications. The entire tibia was visible in most slides, permitting examination of both cortical plates, the implant, marrow spaces, and growth plates at the knee joint. Toluidine blue stains chromatically, so that mature bone stains blue and new bone stains a darker violet. Control samples can be seen in Figs 2 and 3. Samples treated with FGF-1 are displayed in Figs 4 and 5.

Implants treated with FGF-1 showed greater bone-to-implant contact percent (40.3 ± 4.1) than controls (24.9 ± 8.0). This result was significantly different ($P < .01$). Also, bone volume percent associated with the treated implants (11.5 ± 1.3) was almost twice as high as that of controls (6.0 ± 1.0). This difference was significantly different ($P < .005$). Finally, implants treated with FGF-1 showed significantly more nodes of bone calcification than control implants ($P < .05$). Individual areas of analysis (zones) are labeled in Fig 1. Percent bone-to-implant contact,

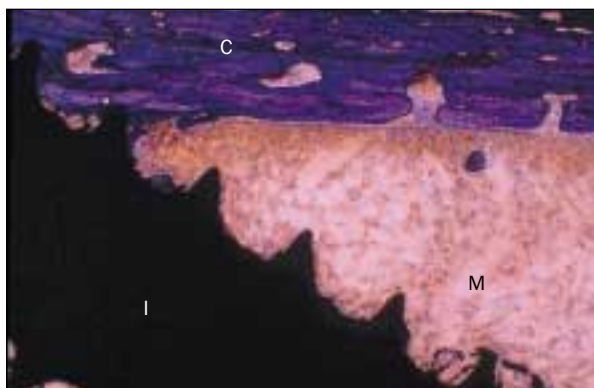


Fig 2 Bone response to control implant. In controls, modest bone growth was associated with implants (I). Below the cortical plate (C), bone can be seen along the surface of the implant. However, little bone is present in the medullary canals (M) (toluidine blue; magnification $\times 40$).



Fig 3 Bone contact in control implant. Bone does not integrate with the implant in this specimen, although not in great amounts. Little bone is seen away from the implant surface (toluidine blue; magnification $\times 100$).

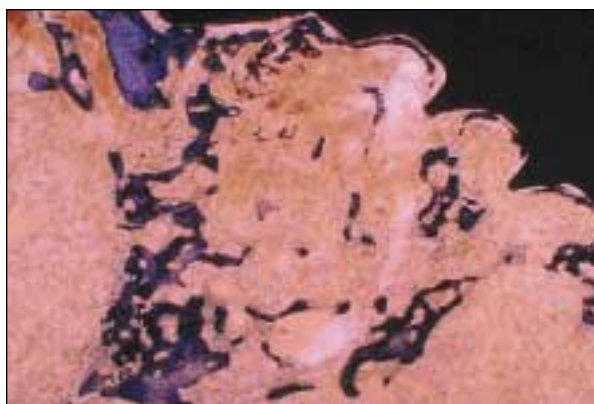


Fig 4 Bone response around implant treated with FGF-1. The bone growth associated with implants treated with FGF-1 is typically greater than controls. The bone is seen further from the implant surface, and more nodules of bone ossification are present. Typically, the greater volume of bone may be attributed to more centers of ossification and, in some cases, larger centers of ossification (toluidine blue; magnification $\times 40$).

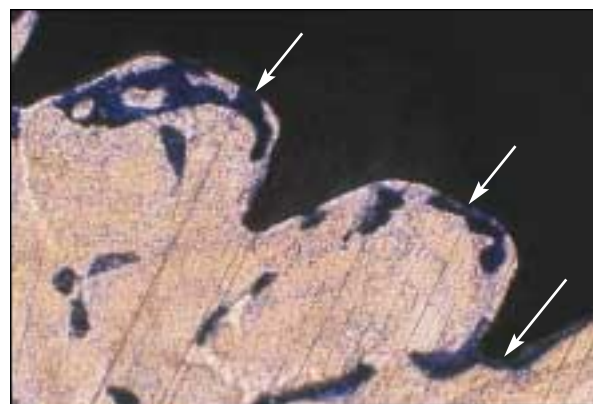


Fig 5 Integration of implant treated with FGF-1. Implants placed with FGF-1 showed increased bone-to-implant contact (arrows). Also, more frequent areas of contact are noted compared to controls. An increase in medullary bone is also evident in this slide (toluidine blue; magnification $\times 100$).

bone volume, and contacting count measurements are provided in Table 2. Total bone-to-implant contact and total bone volume are displayed graphically in Fig 6 and Fig 7, respectively.

Examples of Tc-99m-MDP whole-body and leg images are displayed in Figs 8 and 9. The whole-body images show the retained radioactivity in the skeleton, while the leg images show a close-up view of the joint and implant region. Areas of greater Tc-99m-MDP activity are represented by darker colors. Implants treated with FGF-1 showed significantly more associated Tc-99m-MDP activity than implants alone (Fig 10). The activity (counts/pixel) associated with FGF-treated implants was $9.45 (\pm 0.60)$; the mean activity of control implants was $6.56 (\pm 0.41)$. This result was significantly different ($P < .01$).

Table 2 Results of Histomorphometric Analysis of FGF and Control Groups

Measurement	Control (mean \pm SE)	FGF (mean \pm SE)
Bone-to-implant contact %		
Area no. 1	8.0 \pm 2.6	12.4 \pm 3.0
Area no. 2	17.7 \pm 2.3	30.4 \pm 5.0*
Area no. 3	48.1 \pm 3.9	61.7 \pm 4.1*
Area no. 4	23.6 \pm 2.6	46.5 \pm 5.1†
Area no. 5	29.9 \pm 5.6	39.6 \pm 9.4
Total	24.9 \pm 8.0	40.3 \pm 4.1†
Bone volume %		
Cortical	18.3 \pm 3.2	27.1 \pm 3.8
Medullary	4.1 \pm 0.8	9.2 \pm 1.2†
Total	6.0 \pm 1.0	11.5 \pm 1.3†
Bone nodes contacting implant (n)	16.6 \pm 1.5	22.1 \pm 2.0*

*Statistically significant, $P < .05$; †Statistically significant, $P < .01$.

COPYRIGHT © 2001 BY QUINTESSENCE PUBLISHING CO., INC. PRINTING OF THIS DOCUMENT IS RESTRICTED TO PERSONAL USE ONLY. NO PART OF THIS ARTICLE MAY BE REPRODUCED OR TRANSMITTED IN ANY FORM WITHOUT WRITTEN PERMISSION FROM THE PUBLISHER.

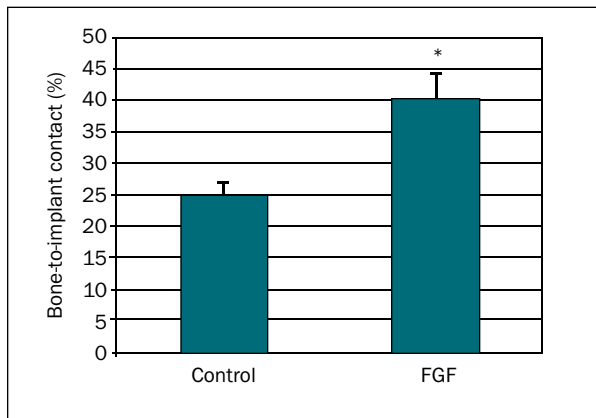


Fig 6 Percent bone-to-implant contact associated with implants (\pm SE). Implants treated with FGF demonstrated significantly more bone-to-implant contact than controls ($*P < .01$).

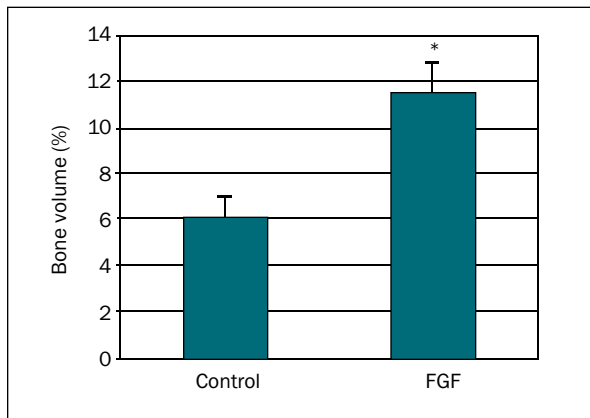


Fig 7 Percent bone volume around implants. Implants treated with FGF-1 demonstrated significantly more associated bone volume ($*P < .005$).



Fig 8 Whole-body Tc-99m-MDP image of rat, dorsal view. Three hours after injection, Tc-99m-MDP is associated with bones and osteoblasts in the skeleton.

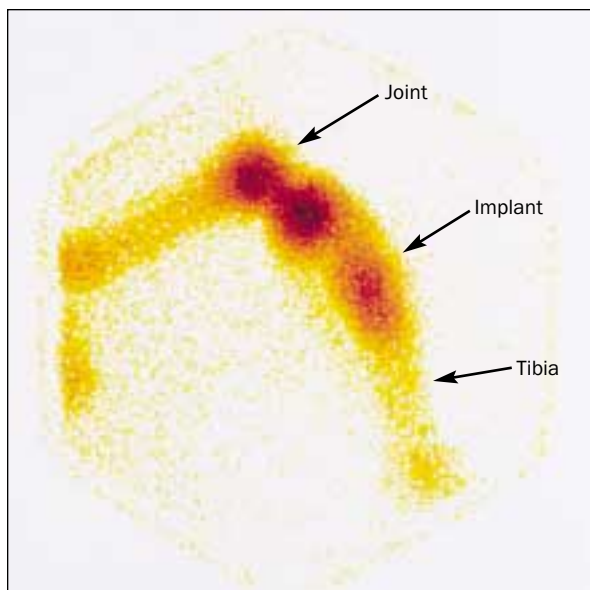


Fig 9 Tc-99m-MDP image of rat leg with implant. Areas of higher osteoblast activity show more intense color, indicating increased action.

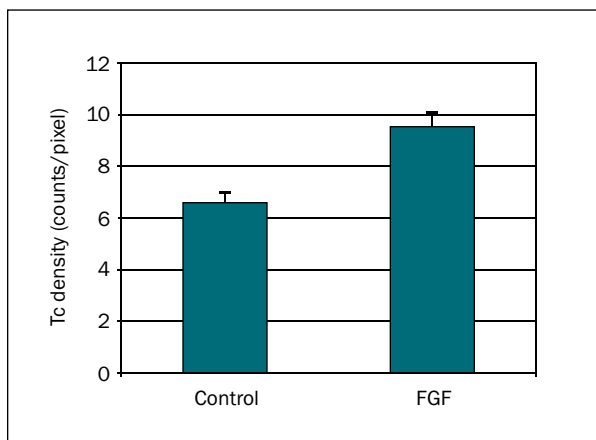


Fig 10 Tc-99m-MDP radioimaging analysis of implants (\pm SE). Implants placed with FGF-1 showed significantly more Tc density than controls ($P < .01$).

DISCUSSION

Biomimetic research using growth factors seems to be a promising area, as the potential for therapeutic treatments using these cytokines increases.^{26–28} Growth factors in the FGF family, especially FGF-1 and FGF-2, have the potential to increase healing in a number of ways. These agents have a proliferative effect on osteoblasts and enhance bone production by increasing the number of cells available to synthesize collagen.^{19,27} In particular, though, FGFs stimulate angiogenesis, a crucial part of the healing process.^{20,29}

The results of this study provide evidence of these effects of FGF-1. Bone-to-implant contact and bone volume percent were clearly greater around implants treated with FGF-1. Also, it was observed when reviewing the slides after histomorphometric analysis that the bone-to-implant contact of FGF-treated implants was greater, not because the bone contacted in larger surface distances per contact, but because contact occurred more frequently. This observation, expressed as bone node count, was statistically significant and represents an important difference between the groups. If the only action of the FGF-1 was to increase only the proliferation of cells already present, the nodes of calcification would be similar in number but larger in the FGF-treated group. The increased number of nodes of ossification, however, may be evidence of increased angiogenesis in the treated samples. The increased nodes of ossification could not exist without a corresponding increase in vascular support. The increase in ossification nodes and the known angiogenic effect of FGF-1 suggest that increased vasculature played a role in the increase of bone associated with FGF-treated implants.

Additionally, the FGF-1 affected the implant site early in the healing process. Only 4 to 6 days after implant placement, implants healing in rat tibiae were characterized by a prolific increase in neovascularization and the appearance of an osteoid seam.²⁴ Technetium-99m-MDP imaging analyses supported the hypothesis that the implants treated with FGF-1 at this point were more advanced in the healing process than controls. The greater uptake of Tc-99m-MDP indicated an increase in osteoblast activity and bone or osteoid deposition. Whether this effect resulted from the angiogenic or proliferative effects of FGF-1 was unclear from these data, though a combination of effects seems likely.

In this study, the addition of FGF-1 to the osteotomy increased percent bone-to-implant contact around the implant, but not in all zones examined. The osteotomy on the medial aspect of the tibia was increased to 2 mm. Since the implant was

only 1.5 mm in diameter, it did not engage the cortical plate in this area (zones 1 and 5). Observation of these zones indicated that the bone did not reach the implant in most cases during the limited healing time of 14 days. Along the opposite cortical plate (zone 3), the FGF did increase bone-to-implant contact. In this region, the bone was much closer to the implant at the time of surgery, as the osteotomy was smaller than the implant, which was screwed into the cortical plate for mechanical stabilization. When treated with FGF-1, the medullary canals (zones 2 and 4) exhibited greater bone-to-implant contact compared to controls—as much as 50% more. This was the area of greatest difference in healing. In the normal healing process, recruitment of cells and the vasculature to support them is the limiting factor in this region. The FGF-1, with its angiogenic and proliferative effects on bone-producing cells, exhibited the greatest effect in these areas, where the biologic infrastructure is more scarce. In the regions of the cortical bone, where osteogenic cells and blood supply are more plentiful and established, the impact of the FGF was not as dramatic, though still statistically significant. These findings agree with the analysis of bone volume surrounding the implants. In specimens treated with FGF-1, bone volume percent was more than twice that of controls.

CONCLUSIONS

This study showed that healing around titanium alloy implants in a rat tibia model was enhanced with an exogenous growth factor, FGF-1. The addition of this growth factor increased bone-to-implant contact associated with the implant, increased the volume of bone associated with the implant, and increased the number of ossification centers touching the implant. Additionally, compared to untreated controls, implants treated with FGF-1 demonstrated increased Tc-99m-MDP binding, as shown by noninvasive gamma camera imaging.

REFERENCES

1. Naert I, Quirynen M, van Steenberghe D, Darius P. A study of 589 consecutive implants supporting complete fixed prostheses. Part II: Prosthetic aspects. *J Prosthet Dent* 1992;68: 949–956.
2. Quirynen M, Naert I, van Steenberghe D, Nys L. A study of 589 consecutive implants supporting complete fixed prostheses. Part I: Periodontal aspects. *J Prosthet Dent* 1992;68: 655–663.
3. Saadoun AP, Le Gall MG. An 8-year compilation of clinical results obtained with Steri-Oss endosseous implants. *Compendium* 1996;17:669–674.

4. Zarb G, Schmitt A. The edentulous predicament II: The longitudinal effectiveness of implant-supported overdentures. *J Am Dent Assoc* 1996;127:66-72.
5. Albrektsson T, Dahl E, Enbom L, et al. Osseointegrated oral implants. A Swedish multicenter study of 8139 consecutively inserted Nobelpharma implants. *J Periodontol* 1988;59:287-296.
6. Misch CE. *Contemporary Implant Dentistry*, ed 2. St Louis: Mosby, 1999.
7. Lynch SE, Buser D, Hernandez RA, et al. Effects of the platelet-derived growth factor/insulin-like growth factor-I combination on bone regeneration around titanium dental implants. Results of a pilot study in beagle dogs. *J Periodontol* 1991;62:710-716.
8. Howes R, Bowness JM, Grotendorst GR, Martin GR, Reddi AH. Platelet-derived growth factor enhances demineralized bone matrix-induced cartilage and bone formation. *Calcif Tissue Int* 1988;42:34-38.
9. Herr G, Hartwig CH, Boll C, Kusswetter W. Ectopic bone formation by composites of BMP and metal implants in rats. *Acta Orthop Scand* 1996;67:606-610.
10. Cole BJ, Bostrom MP, Pritchard TL, et al. Use of bone morphogenetic protein 2 on ectopic porous coated implants in the rat. *Clin Orthop* 1997;219-228.
11. Wang X, Jin Y, Liu B, et al. Tissue reactions to titanium implants containing bovine bone morphogenetic protein: A scanning electron microscopic investigation. *Int J Oral Maxillofac Surg* 1994;23:115-119.
12. Xiang W, Baolin L, Yan J, Yang X. The effect of bone morphogenetic protein on osseointegration of titanium implants. *J Oral Maxillofac Surg* 1993;51:647-651.
13. Yan J, Xiang W, Baolin L, White FH. Early histologic response to titanium implants complexed with bovine bone morphogenetic protein. *J Prosthet Dent* 1994;71:289-294.
14. Kirker-Head CA, Gerhart TN, Armstrong R, Schelling SH, Carmel LA. Healing bone using recombinant human bone morphogenetic protein 2 and copolymer. *Clin Orthop* 1998 Apr;(349):205-217.
15. Gerhart TN, Kirker-Head CA, Kriz MJ, et al. Healing segmental femoral defects in sheep using recombinant human bone morphogenetic protein. *Clin Orthop* 1993 Aug;(293):317-326.
16. Marden LJ, Hollinger JO, Chaudhari A, Turek T, Schaub RG, Ron E. Recombinant human bone morphogenetic protein-2 is superior to demineralized bone matrix in repairing craniotomy defects in rats. *J Biomed Mater Res* 1994;28:1127-1138.
17. Ono I, Ohura T, Murata M, Yamaguchi H, Ohnuma Y, Kuboki Y. A study on bone induction in hydroxyapatite combined with bone morphogenetic protein. *Plast Reconstr Surg* 1992;90:870-879.
18. Mason JJ. The ins and outs of fibroblast growth factors. *Cell* 1994;78:547-552.
19. Gospodarowicz D, Neufeld G, Schweigerer L. Fibroblast growth factor. *Mol Cell Endocrinol* 1986;46:187-204.
20. Slavin J. Fibroblast growth factors: At the heart of angiogenesis. *Cell Biol Int* 1995;19:431-444.
21. Gospodarowicz D, Ferrara N, Schweigerer L, Neufeld G. Structural characterization and biological functions of fibroblast growth factor. *Endocrinol Rev* 1987;8:95-114.
22. Aspenberg P, Tagil M, Kristensson C, Lidin S. Bone graft proteins influence osteoconduction. A titanium chamber study in rats. *Acta Orthop Scand* 1996;67:377-382.
23. Sela J, Shani J, Kohavi D, et al. Uptake and biodistribution of ^{99m}technetium methylene-[³²P] diphosphonate during endosteal healing around titanium, stainless steel and hydroxyapatite implants in rat tibial bone. *Biomaterials* 1995;16:1373-1380.
24. Masuda T, Salvi GE, Offenbacher S, Felton DA, Cooper LF. Cell and matrix reactions at titanium implants in surgically prepared rat tibiae. *Int J Oral Maxillofac Implants* 1997;12:472-485.
25. Donath K, Breuner G. A method for the study of undecalcified bones and teeth with attached soft tissues. The Sage-Schliff (sawing and grinding) technique. *J Oral Pathol* 1982;11:318-326.
26. Robinson CJ. Growth factors: Therapeutic advances in wound healing. *Ann Med* 1993;25:535-538.
27. Lind M. Growth factors: Possible new clinical tools. A review. *Acta Orthop Scand* 1996;67:407-417.
28. Meyer-Ingold W. Wound therapy: Growth factors as agents to promote healing. *Trends Biotech* 1993;11:387-392.
29. Kiritsy CP, Lynch AB, Lynch SE. Role of growth factors in cutaneous wound healing: A review. *Crit Rev Oral Biol Med* 1993;4:729-760.
30. Wang JS, Aspenberg P. Basic fibroblast growth factor enhances bone-graft incorporation: Dose and time dependence in rats. *J Orthop Res* 1996;14:316-323.
31. Aspenberg P, Albrektsson T, Thoringren KG. Local application of growth-factor IGF-1 to healing bone. Experiments with a titanium chamber in rabbits. *Acta Orthop Scand* 1989;60:607-610.
32. Schliephake H, Jamil MU, Knebel JW. Experimental reconstruction of the mandible using polylactic acid tubes and basic fibroblast growth factor in alloplastic scaffolds. *J Oral Maxillofac Surg* 1998;56:616-626.
33. Wiltfang J, Merten HA. Ectopic bone formation with the help of growth factor β FGF. *J Craniomaxillofac Surg* 1996;24:300-304.
34. Rodan SB, Wesolowski G, Thomas K, Rodan GA. Growth stimulation of rat calvaria osteoblastic cells by acidic fibroblast growth factor. *Endocrinology* 1987;121:1917-1923.
35. Bland YS, Critchlow MA, Ashhurst DE. Exogenous fibroblast growth factors-1 and -2 do not accelerate fracture healing in the rabbit. *Acta Orthop Scand* 1995;66:543-548.
36. Nakamura T, Hanada K, Tamura M, et al. Stimulation of endosteal bone formation by systemic injections of recombinant basic fibroblast growth factor in rats. *Endocrinology* 1995;136:1276-1284.
37. Mayahara H, Ito T, Nagai H, et al. In vivo stimulation of endosteal bone formation by basic fibroblast growth factor in rats. *Growth Factors* 1993;9:73-80.